Low loading ORR selectivity evaluation of Pt-free catalysts with scanning electrochemical microscopy

Ndrina Limani, Alice Boudet, Emmanuel Scorsone, Vincent Derycke, Bruno Jousselme, Renaud Cornut

Electrochemistry Communications 153 (2023) 107538

Contents lists available at ScienceDirect

Electrochemistry Communications

journal homepage: www.elsevier.com/locate/elecom

Low loading ORR selectivity evaluation of Pt-free catalysts with scanning electrochemical microscopy

Ndrina Limani [a,1,*], Alice Boudet [a,2], Emmanuel Scorsone [b], Vincent Derycke [a], Bruno Jousselme [a], Renaud Cornut [a,*]

[a] Université Paris-Saclay, CEA, CNRS, NIMBE, LICSEN, 91191 Gif-sur-Yvette, France
[b] Université Paris-Saclay, CEA, List, 91191 Gif-sur-Yvette, France

ARTICLE INFO

Keywords:
Atomic force microscopy
Carbon-based catalyst
Oxygen reduction reaction
ORR selectivity
Rotating ring disc electrode
Scanning electrochemical microscopy

ABSTRACT

The challenges associated to oxygen reduction reaction (ORR) electrocatalysis are undoubtedly the most intricate impediments to solve regarding fuel cell vehicle (FCV) commercialization, mainly due to the complexity of this reaction and the scarcity of the required electrocatalysts. The synthesis of non-precious electrocatalysts with high intrinsic selectivity is indeed crucial in this field, but the methodology utilized to come to selectivity conclusions is undeniably equally important. In this work, we demonstrate how the higher required electrode loadings of a Fe-N-MWCNT catalyst in a rotating ring disc electrode (RRDE) prevent access to all of the peroxide produced by the catalyst during ORR. Via a spraying technique, much smaller amounts of the same catalyst were deposited on a flat boron-doped diamond (BDD) and their loading was determined meticulously by atomic force microscopy (AFM). These ultra-low loadings were investigated using scanning electrochemical microscopy (SECM), which revealed higher peroxide production and lower selectivity. This finding may have crucial implications for future ORR investigations in the laboratory, considering the harmful effect peroxide has on the catalyst.

1. Introduction

The significance of setting up an eco-friendly environment, free of harmful and heat-trapping greenhouse gases, is clear to everyone. If, for a start, we can only convert the transportation sector into an environmentally friendly one, we would significantly reduce the overall emissions worldwide. One such means could be FCVs, on which the scientific community has been working for decades. However, progress is currently not at the desired level due to the inherent complexity of such systems and their unaffordable price mainly related to the cathode electrocatalysts. The latter are screened for their catalytic activity in the laboratory mostly with the R(R)DE method and if excellent performance is found, further screening on a membrane electrode assembly (MEA) is required. Regrettably, this step is often a barrier preventing the continuation to further stages.

When investigating Pt-free catalysts with R(R)DE, usually higher amounts of materials are investigated compared to Pt, in order to compensate for their lower intrinsic activity. The thick catalyst layers often tend to hide the real electrochemical response. Indeed, in previous works it has been pointed out that the performance of MEA and RRDE differs considerably, with RRDE results highly overestimating the ORR performance [1]. Certainly, these two investigation methods have their differences, however, the catalyst ought to have an intrinsic activity and selectivity that is not significantly dependent on the method used. Therefore, this invokes the question: are we accurately determining the ORR performance at the laboratory scale, or are we too focused on synthesizing novel electrocatalysts? This question is even more pertinent when one considers that in addition to RRDE, there are other lab-scale methods able to investigate ORR performance, unfortunately underused by the community.

SECM is a valuable tool in electrochemical studies because of the many advantages that microelectrodes can provide [2–4]. Despite the competence of SECM to be employed on its own, curiously in electrocatalysis literature it is vastly used for supporting the RRDE results with

* Corresponding authors.
E-mail addresses: ndrina.limani@cea.fr (N. Limani), renaud.cornut@cea.fr (R. Cornut).
[1] Current address: Analytical Chemistry-Center for Electrochemical Sciences (CES) Faculty of Chemistry and Biochemistry Ruhr University Bochum, Universitätsstraße 150, Bochum, Germany.
[2] Current address: SunErgy, 85-91 Boulevard Alsace-Lorraine F-93110 Rosny-sous-Bois cedex, France.

https://doi.org/10.1016/j.elecom.2023.107538
Received 29 June 2023; Received in revised form 10 July 2023; Accepted 11 July 2023
Available online 12 July 2023

extra information, such as activity maps showing the distribution of current in the catalyst deposit [5,6]. SECM was used hand in hand with RRDE knowing that both are powerful tools for assessing ORR selectivity via peroxide determination. There are works where the RRDE results were concordant with the SECM ones [7,8], and works that showed that RRDE rather overestimates activity [9]. The number of electrons assessment via SECM by employing pulsed-profile is the approach most widely used for ORR selectivity assessment [10,11], although it is not implemented as much as one would expect. Therefore, RRDE still dominates within laboratory-scale techniques for assessing ORR activity and selectivity of the catalyst.

Further SECM research into ORR electrocatalysis is essential in order to unlock its power and better understand the technique and the catalyst itself. In this work, the latent potential of SECM was exploited by studying ultra-low loadings of a Fe-N-MWCNT catalyst, which were not possible to be acquired in a mm-sized electrode in RRDE, via a rigorous loading determination using AFM. This provides a new and clearer insight into the selectivity of the catalyst which is significantly lower than the selectivity usually observed with the same type of catalyst, using RRDE.

2. Materials and methods

The RRDE experimental procedure and ink preparation is depicted in the Supporting Information along with the catalyst deposition method in SECM measurements and the AFM data treatment.

2.1. Catalyst synthesis

The synthesis of the Fe-N-MWCNT catalyst powder used as a model catalyst in this work was done via the following procedure: iron acetate (Alfa Aesar), zinc nitrate (Alfa Aesar) and 2-methylimidazole (Alfa Aesar) (forming a MOF) and carbon nanotubes (NC 7100 from Nanocyl) were mixed 30 min in ethanol. Then, the solvent was removed by evaporation. The powder was subjected to a first pyrolysis at 900 °C for 1 h under argon, followed by a second pyrolysis at 900 °C for 30 min in an NH_3 atmosphere without any acid treatment. Zinc is removed by raising the temperature, leaving behind a porous carbon material. Its characterization with scanning electron microscopy (SEM) and Brunauer–Emmett–Teller (BET) are depicted in Figure S1 and Figure S2.

2.2. Ink preparation for SECM measurements

The catalyst ink was prepared by dispersing 20 mg of catalyst powder into a 1.175 mL mixture of isopropanol and water (3:1 ratio) and 24 μL of Nafion (5% in weight after drying), leading to a concentration of 17 mg/mL. The Nafion content in this formulation is about 5 %. After the addition of ~15 g of Zirconium beads, the ink was treated for 40 min on an IKA ULTRA-TURRAX® Tube Drive for an initial breaking of agglomerates, followed by ball milling for 2 weeks in an IKA ROLLER 6 shaker. The ink was then diluted to ~0.2 g/L and ultrasonicated for at least 30 min prior to depositing it on the substrate.

2.3. BDD substrate

Diamond nanoparticle seeds (MSY 0–0.03 μm GAF, Microdiamant, Switzerland) were firstly deposited onto a silicon substrate, following a procedure published previously. Thereafter, a first 500 nm layer of heavily BDD was grown by microwave-assisted plasma chemical vapor deposition (MPCVD) in a Seki Diamond AX6500 diamond growth reactor in a H2 plasma which contains 1% methane, serving as the carbon source and trimethyl boron serving as the dopant. Then, the substrate was transferred to another Seki Diamond AX6500 diamond growth reactor, in which case a thick layer of 100 μm intrinsic diamond overgrew onto the boron-doped diamond. Ultimately, for obtaining a free-standing diamond film, wet etching was performed to ensure the removal of silicon via a mixture of HF/HNO_3. The smooth surface of BDD is the surface which was originally contacting silicon, which was also smooth.

[12]. The scheme of this procedure is shown in Fig. 1. The substrate was scanned with AFM (image in Fig. 2a) where the root mean square (RMS) roughness was determined to be only 0.281 nm for a 2 μm area. Some small spots appear brighter in the AFM image, however, if we see the section analysis of such region in Fig. 2b (marked with a black line in Fig. 2a), we can see that even such irregularity exhibits a roughness of less than 3 nm. The catalyst spots are 200μm whose optical micrographs are shown in Figure S7.

2.4. SECM approach

The common ultramicroelectrode (UME) material of choice for ORR investigation is Pt [13] due to its high activity towards ORR, while the experiments are usually carried out in redox competition (RC) mode, which is a valuable protocol for ORR studies as it excludes background currents often encountered in tip generation/substrate collection (TG/SC) mode [13,14]. It was demonstrated by Henrotte et al. that Au probes are an excellent alternative for ORR investigation due to their higher sensitivity towards O_2 detection and higher stability which allows steady state measurements to be performed [15,16]. For H_2O_2 detection, however, Pt UME remains the best choice. Consequently, the SECM experiments herein were originally performed with a new approach using two UMEs subsequently, namely an Au UME for ORR detection in RC mode and a Pt UME for H_2O_2 oxidation in substrate generation/tip collection (SG/TC) mode (Fig. 3). The UMEs were purchased from Sensolytics, both with a 10 μm diameter, RG ~ 10 and r_T ~ 5 μm. A SCE electrode was used as the reference electrode (RE) and a Pt mesh separated from the electrolyte by glassware was used as the counter electrode (CE).

The tip-to-substrate distance (d) used was 30 μm, which was achieved via the negative feedback approach. As the tip approaches the substrate, the current keeps decreasing and this decrease stops when the tip touches the substrate due to complete oxygen depletion. At this point we record the Z coordinate as 0, and then go up 30 μm. Prior to the start of each experiment, the electrolyte (0.05 M H_2SO_4) was purged with oxygen for at least 15 min, and then the O_2 flow was kept on top of the electrolyte while avoiding bubbles. Before starting the electrochemical measurements, the tip was positioned over the centre of the deposit, which was achieved via linescans in RC mode ORR, as follows: the sample was polarized at a potential which reduces oxygen, and the Au tip as well. We start the linescan with the tip above the BDD in which case we have high current (no ORR activity, tip detecting the oxygen). As we move linearly approaching the catalyst, the current starts to deplete due to the competition of oxygen consumption between the catalyst and the tip (net ORR current regarding the catalyst increases). When the current cannot deplete anymore, as all the oxygen is consumed in the vicinity (max ORR), we assume that this is the center of the catalyst (Fig. 4). Once the center is found, we leave the tip there, and we record the tip position coordinates in case we need to find the center again. Note that the catalyst spots are visible on the camera, this procedure concerns just finding the very center of the catalyst.

During the measurements, the Au tip was held static above the deposit and polarized at −0.65 V vs SCE for oxygen reduction, while the substrate was swept at potentials from 0.4 V to −0.3 V vs SCE at a scan rate of only 2 mV/s to achieve steady state conditions. Subsequently, for peroxide detection the substrate was swept at the same potential range as for ORR, while at the Pt UME a chronoamperogram (CA) was recorded at 1.1 V vs SCE for H_2O_2 oxidation. The tip currents acquired by both experiments were used to calculate the n via Eq. (1) [9], which is similar to the way we calculate n in RRDE experiments (Supporting Information), except that here the background current is corrected, namely the current at all potentials is subtracted by the current value at the most positive potential at which ORR does not occur. The collection efficiency

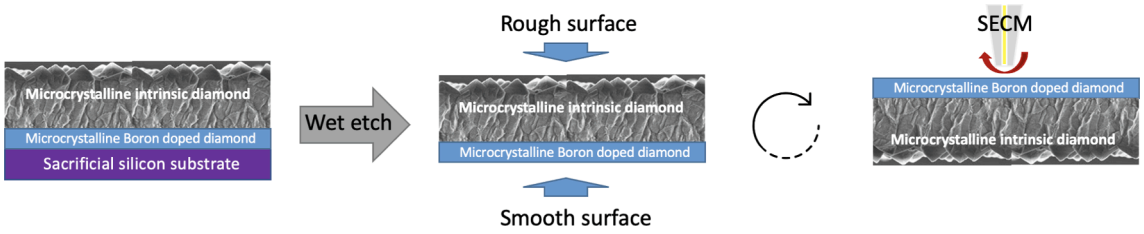

Fig. 1. Scheme showing the fabrication process of BDD.

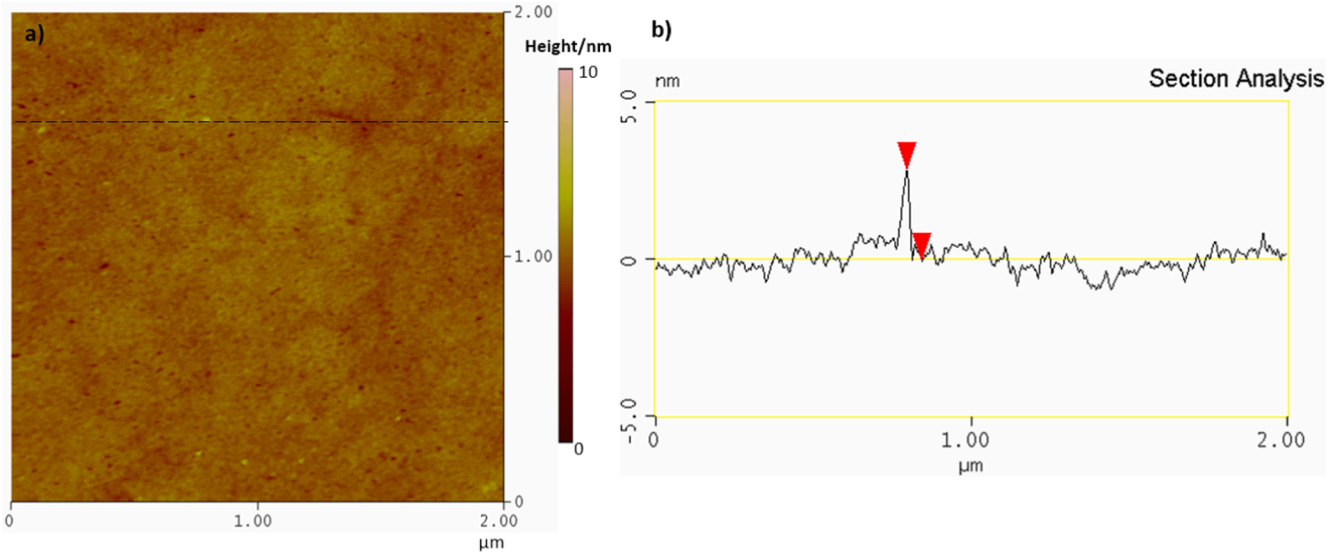

Fig. 2. A) afm image of the flat bdd substrate, b) section analysis of the region marked with a black line in the image, depicting the roughness of the white spots in the image.

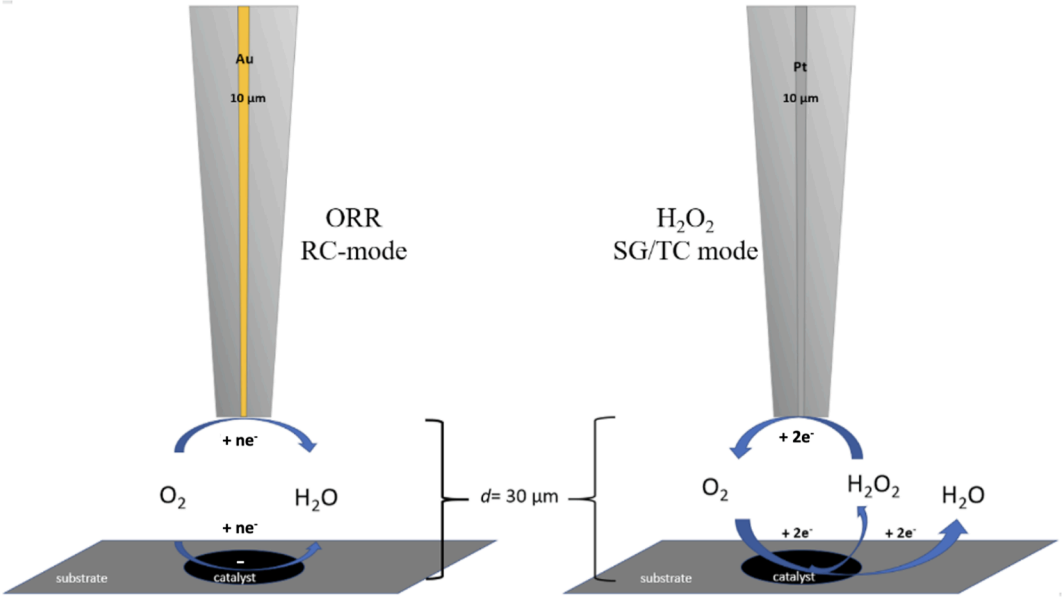

Fig. 3. Scheme of the dual electrode SECM approach used.

(*N*) is commonly taken as 100% as long as the probe current does not vary with a change in *d* [9,17] as it was found in our case. However, considering that two different electrodes are employed herein, which may have slight dimensional variations, numerical simulations were performed previously in our group, in which case the collection efficiency of both tips, Pt in SG/TC mode and Au in RC mode, were taken into account ($N = \eta_{RC}/\eta_{SG/TC}$) [18]. The collection efficiency for both tips, at the same experimental parameters as used in this work (*d*, RG, r_T), was $N = \frac{4.3\%}{3.7\%} \approx 100\%$[18].

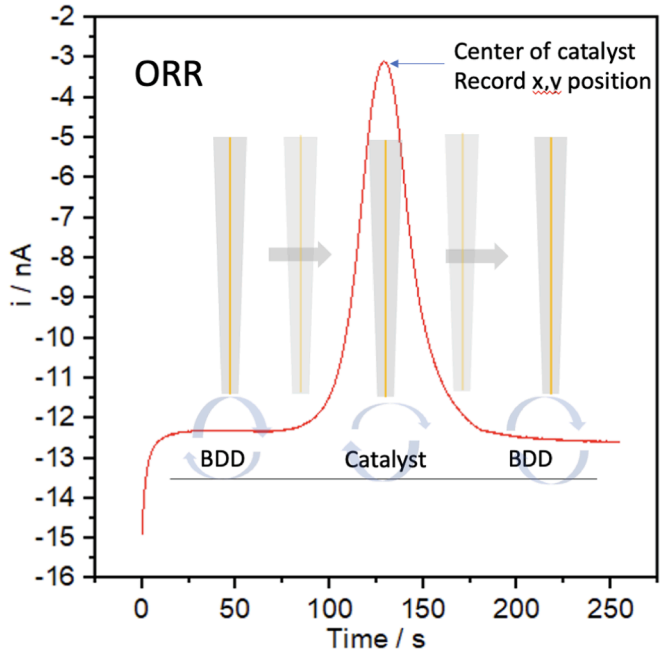

Fig. 4. Linescan in RC mode for evaluating the position of center of the catalyst.

$$n = 4 \times \frac{\Delta i_{O_2}}{\left(\frac{\Delta i_{H_2O_2}}{N}\right) + \Delta i_{O_2}} \quad (1)$$

3. Results and discussion

Initially, the Fe-N-MWCNT catalyst at different electrode loadings was studied via RRDE, with the ORR response shown in Fig. 5b along with the currents detected at the Pt ring simultaneously, in Fig. 5a. The selectivity with the $\%H_2O_2$ and n at different potentials are shown in Fig. 6. The percentage of peroxide detected is as low as 3% at the highest loading and ~32% at the lowest loading, while the n varies from ~3.42 to 3.95 at ~0.63 V vs RHE respectively. Higher peroxide detection for lower loaded deposits is consistent with what has been observed previously for carbon-based materials [19–22]. This was attributed to the larger diffusion path of H_2O_2 in thicker layers, possibly leading to a

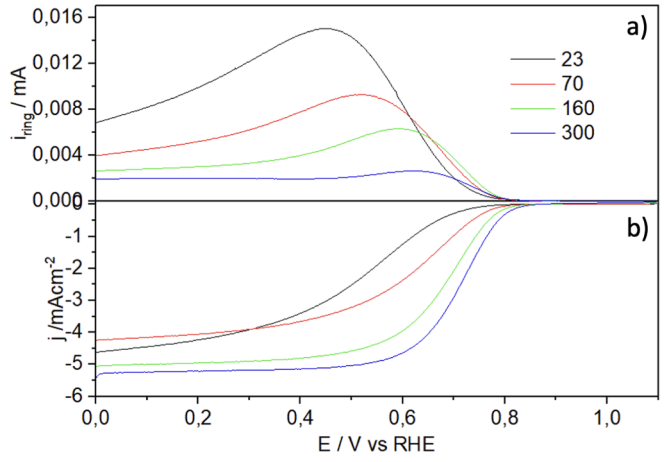

Fig. 5. A) Current detected at the Pt ring vs the potential applied at the disc for different loadings (μg/cm^2), b) the corresponding LSVs at the glassy carbon disc. Experiments obtained for bm-ink of Fe-N-MWCNT catalyst in O_2 saturated 0.05 M H_2SO_4 at a scan rate of 5 mV/s, corresponding to the measurement at 1600 rpm.

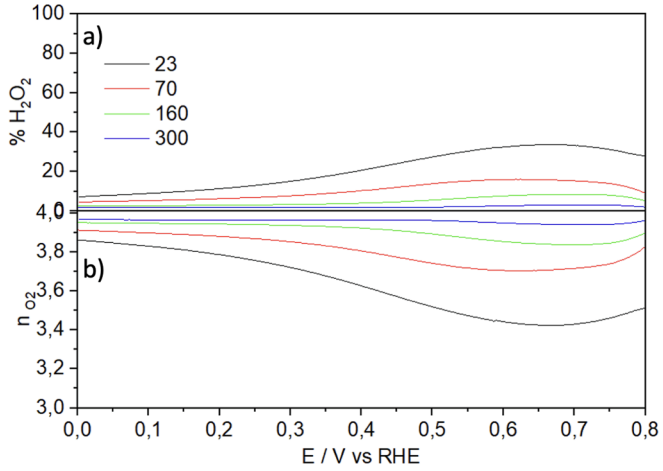

Fig. 6. A) peroxide percentage detected at the pt ring vs the potential applied at the disc for different loadings (μg/cm^2), b) the corresponding n values. Experiments obtained for us-ink of Fe-N-MWCNT catalyst in O_2 saturated 0.05 M H_2SO_4 at a scan rate of 5 mV/s, corresponding to the measurement at 1600 rpm.

further electrochemical or chemical reduction of H_2O_2 to H_2O within the layer before being released into the electrolyte [23]. Peroxide disproportionation to O_2 and H_2O within the layer is also possible [24]. However, this variation in selectivity makes it difficult to come to a conclusion as to what is the intrinsic n of the catalyst. It could be interesting to see at what point the peroxide would stop increasing while one decreases the loading, however, lower loadings were not possible to be studied with RRDE due to limitations in electrode coverage (Figure S6).

3.1. SECM measurements

The RRDE limitation has been overcome by using SECM as a microscale technique which allows the study of lower loadings. The BDD was previously proven to be inert to ORR up to −0.3 V vs SCE [15], and in our experiments we always asses the background (substrate) current similarly to Fig. 4, and subtract it from the net ORR and H_2O_2 currents. The ORR was studied in RC mode, and the probe current normalized by its value at the most positive potentials where no ORR occurs, shows the ORR catalytic activity versus applied potential, acquired via the Au UME at a d of 30 μm (Fig. 7). At more cathodic potentials both the sample and the Au tip compete for ORR, resulting in a reduced current at the tip as the potential becomes more negative. The more the current depletes, the higher the activity of the catalyst towards ORR. From Fig. 7, it can be seen that at higher catalyst loadings more oxygen is consumed by the catalyst and the net ORR current is increased. It can also be recognized that the overpotentials are higher in the SECM results compared to RRDE for similar loadings. This is not very surprising considering that the agglomerate scale in RRDE and SECM deposits is not the same due to different deposition methods, the latter possibly having big agglomerates with hindered active sites. Besides, in RRDE the ORR is measured directly at the GC electrode with the catalyst on it, while in SECM this is an indirect measurement of the oxygen depletion in the vicinity.

Nevertheless, in order to acquire the selectivity or number of transferred electrons the peroxide was determined via the SG/TC mode, where the H_2O_2 detected increases at more cathodic potentials due to a higher rate of oxygen reduction at the catalyst, leading to a higher current at the Pt tip (Fig. 8a). Here, less peroxide is detected at the highest loading (0.15nA) and larger H_2O_2 current is detected at the lowest loading (1.25nA). Using the ORR and H_2O_2 background-corrected currents, the n was determined for all loadings as shown in Fig. 8b. All curves seem to exhibit a n roughly independent of potential in a wide range (0 to ~0.5 V vs RHE), with the exception of the 5.7 μg/

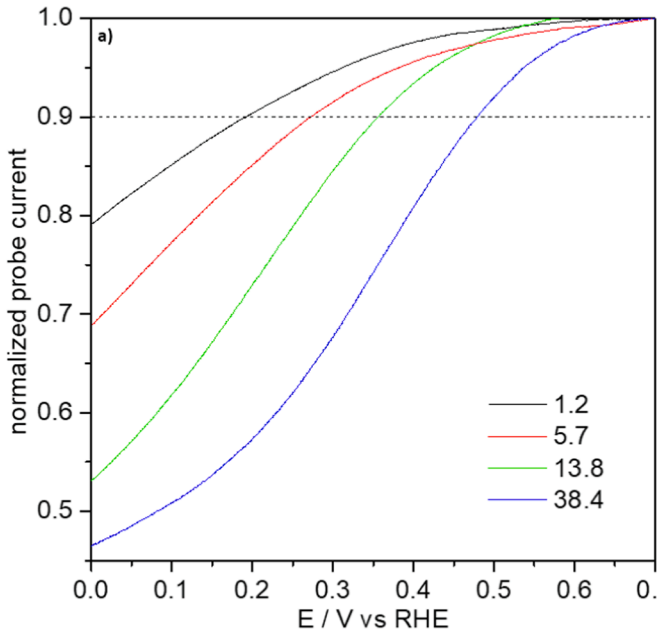

Fig. 7. Normalized probe current acquired via RC mode of SECM, versus applied potential at the sample. Results correspond to all studied loadings in μg/cm^2. Electrolyte used was 0.05 M H_2SO_4 saturated with O_2, Au UME 10 μm, d = 30 μm and BDD substrate.

cm^2 deposit, which has a less steady behaviour. As predicted by the trend of the H_2O_2 currents, the number of electrons increased with loading. At 0 V vs RHE the most loaded deposit (38.4 μg/cm^2) exhibits a $n \sim 3.9$, followed by 13.8 μg/cm^2 with $n \sim 3.8$, 5.7 μg/cm^2 deposit with $n \sim 3.3$ and finally, the 1.2 μg/cm^2 deposit has a n of only 2.6. The latter suggests that this catalyst undergoes ORR via a pathway which is close to 2 electrons, contrary to the highest loadings which suggest a ~ 4 electron pathway.

3.2. AFM measurements on the SECM studied deposits

To explain the differences in peroxide detected at different loadings, we zoomed further into the agglomerates of the deposits via AFM. The agglomerate size of the deposits is plotted against their contribution to the total volume (Fig. 9a) with the procedure depicted in Supporting Information. It can be seen that the 38.4 μg/cm^2 deposit contains particles in a range of 20–40 μm^3, corresponding to 7% of the total volume, particles of 70–80 μm^3 corresponding to 5% of the total volume and 90–110 μm^3 to 4%, in addition to the smaller ones from 0 to 20 μm^3 the sum of which makes up for the rest of the contribution (84%). It is followed by the 13.8 μg/cm^2 deposit with particle volumes of 19–30 μm^3 and 0–11 μm^3 particles. The 5.7 μg/cm^2 deposit has particles up to 14 μm^3 and the lowest loaded deposit has particles with a volume up to 3 μm^3. There is a clear trend on the agglomerate size increase with loading which was rather qualitatively evident as well from the AFM images (Figure S7). This is possibly a consequence of material accumulation at the substrate as the ink evaporates during the spraying process. For larger agglomerates, the diffusion path of the intermediate may be longer, possibly leading to peroxide decomposition before release in the solution. In this way, less peroxide could be detected at the Pt UME, leading to an apparent higher number of electrons transferred. In the case of small agglomerates at the lowest loadings, a volume of only ~ 3 μm^3 might be already small enough for the intermediate formed inside to be easily released onto the electrolyte and thus get detected by the electrode. This trend is consistent with what was previously observed in a SECM loading/activity study [9].

4. Conclusion

In this work, the ORR selectivity and the agglomerate scale of a Fe-N-MWCNT catalyst were investigated by RRDE, SECM and AFM respectively. The loading of all the deposits was unambiguously determined by doing AFM scans prior to the SECM measurement where the agglomerate volume was extracted as well. While in RRDE measurements, the lowest number of electrons observed was 3.2, in SECM at a loading of 1.2 μg/cm^2 a n of only 2.6 was acquired. Therefore, there is more peroxide produced at the sample that one might have thought solely from the RRDE measurements where this information could have been hidden, especially if one would focus on the highest loadings. In other words, the intrinsic selectivity of this catalyst seems to be closer to the 2 electron pathway. This outcome is very significant when considering the integration of the catalyst into a fuel cell, as a high amount of peroxide leads to catalyst degradation. However, even in the SECM experiments the n still continued varying with loading. Via AFM we observed a correlation between big agglomerate size and smaller H_2O_2 currents (therefore higher n). It appears that larger agglomerates lead to peroxide entrapment. Nevertheless, the ability to study ultra-low loadings in SECM is valuable as we can get closer to the intrinsic number of transferred electrons, so, if at such low loadings there is still few or no peroxide detected, this serves as an assurance that the catalyst is

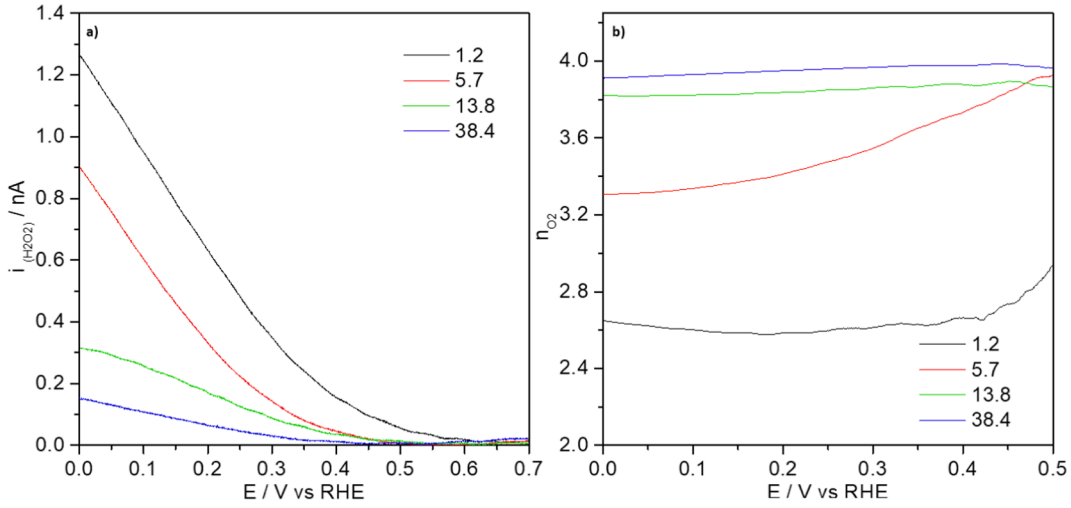

Fig. 8. A) net background corrected h_2O_2 currents acquired with a 10 μm Pt UME in SG/TC mode at d = 30 μm, b) number of transferred electrons calculated from the ORR and H_2O_2 currents while considering N = 100%. Results correspond to all studied loadings in μg/cm^2. Electrolyte used was 0.05 M H_2SO_4 saturated with O_2.

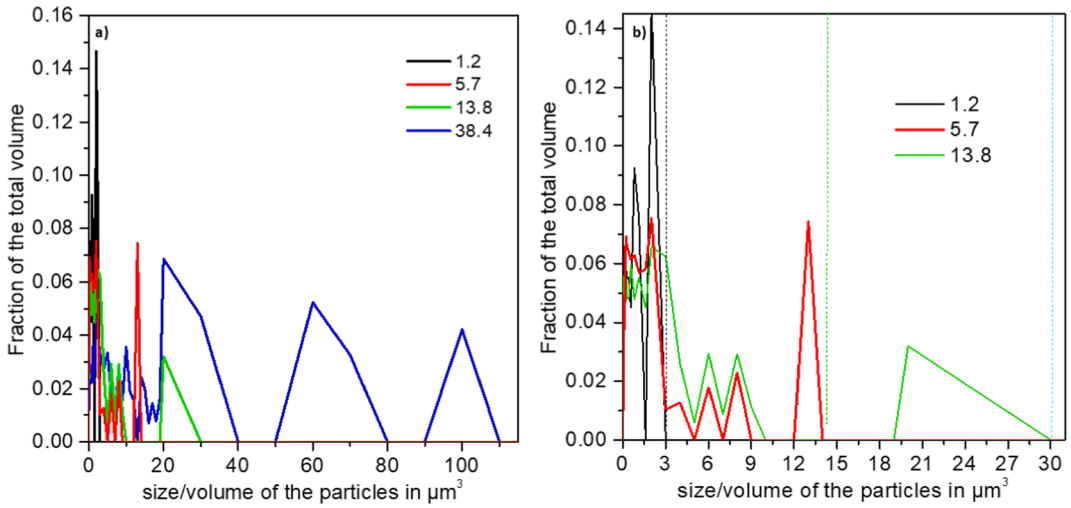

Fig. 9. A) particle sizes and their distribution determined by afm for all loadings in μg/cm^2, b) particle sizes and their distribution for three loadings excluding the highest (zoomed in).

selective for ORR. These results also suggest that, in future works, it is critical that the catalyst deposit is more rigorously homogeneous with small agglomerates so that the entrapment of peroxide within the layer could be avoided and one could get access to the core number of transferred electrons.

Declaration of Competing Interest

The authors declare that they have no known competing financial interests or personal relationships that could have appeared to influence the work reported in this paper.

Data availability

Data will be made available on request.

Acknowledgements

The authors acknowledge the SENTINEL project funded by European Union Horizon 2020 research and Innovation (Marie Skłodowska-Curie MSCA-ITN) under the grant agreement no. 812398 and the PEGASUS project, funded by the European Union Horizon 2020 research and innovation program FCH-01-2-2017, no. 779550.

Appendix A. Supplementary data

Supplementary data to this article can be found online at https://doi.org/10.1016/j.elecom.2023.107538.

References

[1] J. Fan, M. Chen, Z. Zhao, Z. Zhang, S. Ye, S. Xu, H. Wang, H. Li, Bridging the gap between highly active oxygen reduction reaction catalysts and effective catalyst layers for proton exchange membrane fuel cells, Nat. Energy 6 (2021) 475–486, https://doi.org/10.1038/s41560-021-00824-7.

[2] L.E. Strange, X. Li, E. Wornyo, M. Ashaduzzaman, S. Pan, Scanning electrochemical microscopy for chemical imaging and understanding redox activities of battery materials, Chemical & Biomedical, Imaging 1 (2023) 110–120, https://doi.org/10.1021/cbmi.3c00014.

[3] R. He, L. Zhou, R. Tenent, M. Zhou, Basics of the scanning electrochemical microscope and its application in the characterization of lithium-ion batteries: a brief review, Mater. Chem. Front. 7 (2023) 662–678, https://doi.org/10.1039/D2QM01079H.

[4] T. Kai, C.G. Zoski, A.J. Bard, Scanning electrochemical microscopy at the nanometer level, Chem. Commun. 54 (2018) 1934–1947, https://doi.org/10.1039/C7CC09777H.

[5] V. Singh, A. Tiwari, T.C. Nagaiah, Facet-controlled morphology of cobalt disulfide towards enhanced oxygen reduction reaction, Journal of Materials Chemistry A 6 (2018) 22545–22554, https://doi.org/10.1039/C8TA06710D.

[6] A. Tiwari, V. Singh, D. Mandal, T.C. Nagaiah, Nitrogen containing carbon spheres as an efficient electrocatalyst for oxygen reduction: Microelectrochemical investigation and visualization, Journal of Materials Chemistry A 5 (2017) 20014–20023, https://doi.org/10.1039/C7TA05503J.

[7] A. Tiwari, V. Singh, T.C. Nagaiah, Tuning the $MnWO_4$ morphology and its electrocatalytic activity towards oxygen reduction reaction, Journal of Materials Chemistry A 6 (2018) 2681–2692, https://doi.org/10.1039/C7TA10380H.

[8] B. Sidhureddy, S. Prins, J. Wen, A.R. Thiruppathi, M. Govindhan, A. Chen, Synthesis and electrochemical study of mesoporous nickel-cobalt oxides for efficient oxygen reduction, ACS Applied Materials & Interfaces 11 (2019) 18295–18304, https://doi.org/10.1021/acsami.8b22351.

[9] A. Dobrzeniecka, A.R. Zeradjanin, J. Masa, M. Blicharska, D. Wintrich, P.J. Kulesza, W. Schuhmann, Evaluation of kinetic constants on porous, non-noble catalyst layers for oxygen reduction—A comparative study between SECM and hydrodynamic methods, Catalysis Today 262 (2016) 74–81, https://doi.org/10.1016/j.cattod.2015.07.043.

[10] G. Seiffarth, M. Steimecke, T. Walther, M. Kühhirt, S. Rümmler, M. Bron, Mixed transition metal oxide supported on nitrogen doped carbon nanotubes – a simple bifunctional electrocatalyst studied with scanning electrochemical microscopy, Electroanalysis 28 (2016) 2335–2345, https://doi.org/10.1002/elan.201600254.

[11] X. Chen, A.J.R. Botz, J. Masa, W. Schuhmann, Characterisation of bifunctional electrocatalysts for oxygen reduction and evolution by means of SECM, Journal of Solid State Electrochemistry 20 (2016) 1019–1027, https://doi.org/10.1007/s10008-015-3028-z.

[12] N. Limani, E. Batsa Tetteh, M. Kim, T. Quast, E. Scorsone, B. Jousselme, W. Schuhmann, R. Cornut, Scrutinizing intrinsic oxygen reduction reaction activity of a Fe−N−C catalyst via scanning electrochemical cell microscopy, ChemElectroChem 10 (2023) e202201095.

[13] N. Limani, A. Boudet, N. Blanchard, B. Jousselme, R. Cornut, Local probe investigation of electrocatalytic activity, Chemical Science 12 (2021) 71–98, https://doi.org/10.1039/D0SC04319B.

[14] K. Eckhard, X. Chen, F. Turcu, W. Schuhmann, Redox competition mode of scanning electrochemical microscopy (RC-SECM) for visualisation of local catalytic activity, Physical Chemistry Chemical Physics 8 (2006) 5359, https://doi.org/10.1039/b609511a.

[15] O. Henrotte, A. Boudet, N. Limani, P. Bergonzo, B. Zribi, E. Scorsone, B. Jousselme, R. Cornut, Steady-state electrocatalytic activity evaluation with the redox competition mode of scanning electrochemical microscopy: A gold probe and a boron-doped diamond substrate, ChemElectroChem. 7 (2020) 4633–4640, https://doi.org/10.1002/celc.202001088.

[16] A. Boudet, O. Henrotte, N. Limani, F. El Orf, F. Oswald, B. Jousselme, R. Cornut, Unraveling the link between catalytic activity and agglomeration state with scanning electrochemical microscopy and atomic force microscopy, Anal. Chem. 94 (2022) 1697–1704, https://doi.org/10.1021/acs.analchem.1c04256.

[17] A. Dobrzeniecka, A. Zeradjanin, J. Masa, A. Puschhof, J. Stroka, P.J. Kulesza, W. Schuhmann, Application of SECM in tracing of hydrogen peroxide at multicomponent non-noble electrocatalyst films for the oxygen reduction reaction, Catalysis Today 202 (2013) 55–62, https://doi.org/10.1016/j.cattod.2012.03.060.

[18] A. Boudet, Investigation of platinum-free ORR catalysts at agglomerate scale: from local probe characterizations to modeling studies, (2021). https://www.theses.fr/2021UPASF037.

[19] A. Bonakdarpour, M. Lefevre, R. Yang, F. Jaouen, T. Dahn, J.-P. Dodelet, J.R. Dahn, Impact of loading in RRDE experiments on Fe–N–C Catalysts: Two- or four-electron

oxygen reduction? Electrochem. Solid-State Lett. 11 (2008) B105, https://doi.org/10.1149/1.2904768.
[20] E.J. Biddinger, D. von Deak, D. Singh, H. Marsh, B. Tan, D.S. Knapke, U.S. Ozkan, Examination of catalyst loading effects on the selectivity of CN_x and Pt/VC ORR catalysts using RRDE, J. Electrochem. Soc. 158 (2011) B402, https://doi.org/10.1149/1.3552944.
[21] G. Zhang, Q. Wei, X. Yang, A.C. Tavares, S. Sun, RRDE experiments on noble-metal and noble-metal-free catalysts: Impact of loading on the activity and selectivity of oxygen reduction reaction in alkaline solution, Applied Catalysis B: Environmental 206 (2017) 115–126, https://doi.org/10.1016/j.apcatb.2017.01.001.
[22] E.S.F. Cardoso, G.V. Fortunato, G. Maia, Use of rotating ring-disk electrodes to investigate graphene nanoribbon loadings for the oxygen reduction reaction in alkaline medium, ChemElectroChem. 5 (2018) 1691–1701, https://doi.org/10.1002/celc.201800331.
[23] M. Bron, S. Fiechter, P. Bogdanoff, H. Tributsch, Thermogravimetry/mass spectrometry investigations on the formation of oxygen reduction catalysts for PEM fuel cells on the basis of heat-treated iron phenanthroline complexes, Fuel Cells 2 (2002) 137–142, https://doi.org/10.1002/fuce.200290012.
[24] C.H. Choi, H.C. Kwon, S. Yook, H. Shin, H. Kim, M. Choi, Hydrogen peroxide synthesis via enhanced two-electron oxygen reduction pathway on carbon-coated Pt surface, J. Phys. Chem. C 118 (2014) 30063–30070, https://doi.org/10.1021/jp5113894.